

Orthogonal Rendezvous Routing Protocol for Wireless Mesh Networks

Bow-Nan Cheng, *Member, IEEE*, Murat Yuksel, *Member, IEEE*, and Shivkumar Kalyanaraman, *Senior Member, IEEE*

Abstract—Routing in multi-hop wireless networks involves the *indirection* from a *persistent name (or ID)* to a *locator*. Concepts such as coordinate space embedding help reduce the number and dynamism complexity of bindings and state needed for this indirection. Routing protocols which do not use such concepts often tend to flood packets during route discovery or dissemination, and hence have limited scalability. In this paper, we introduce Orthogonal Rendezvous Routing Protocol (ORRP) for meshed wireless networks. ORRP is a lightweight-but-scalable routing protocol utilizing *directional communications* (such as directional antennas or free-space-optical transceivers) to relax information requirements such as coordinate space embedding and node localization. The ORRP source and ORRP destination send route discovery and route dissemination packets respectively in locally-chosen orthogonal directions. Connectivity happens when these paths intersect (i.e., rendezvous). We show that ORRP achieves connectivity with high probability even in sparse networks with voids. ORRP scales well without imposing DHT-like graph structures (eg: trees, rings, torus etc). The total state information required is $O(N^{3/2})$ for N -node networks, and the state is uniformly distributed. ORRP does not resort to flooding either in route discovery or dissemination. The price paid by ORRP is suboptimality in terms of path stretch compared to the shortest path; however we characterize the average penalty and find that it is not severe.

Index Terms—Directional antennas, free-space-optics, wireless mesh, wireless routing protocol.

I. INTRODUCTION

WIRELESS mesh networks have attracted interest because they can complement the cellular model and expand wireless reach in metro-broadband deployment [20]. Routing in multi-hop wireless networks has grappled with the twin requirements of connectivity and scalability. Early MANET protocols such as DSR [9], DSDV [7], AODV [8], among others, explored proactive and reactive routing methods which either flood information during route dissemination or

Classification of Research Issues in Position-based Schemes

L3: Geographic Routing using Node IDs (e.g. GPSR, TBF)	→	<div style="border: 1px solid black; padding: 5px; text-align: center;"> ORRP </div>
L2: ID to Location Mapping (e.g. GHT, GLS, etc.)		
L1: Node Localization (e.g. GPS Receivers)		
		N/A

Fig. 1. Classification of research issues in position based routing schemes.

route discovery, respectively. Even in mesh networks which are not mobile, link-states need to be flooded more often than in wired networks. Flooding poses an obvious scalability problem. In response, position-based routing paradigms such as GPSR [3] were proposed to reduce the state complexity and control-traffic overhead by leveraging the Euclidean properties of a coordinate space embedding. These schemes require nodes to be assigned a coordinate in the system, and still require a mapping from nodeID to coordinate location. In this paper, we focus on routing with even less information, i.e., scalable, efficient routing without explicit positioning.

A recent trend in wireless communications has been the desire to leverage directional forms of communications (e.g. directional smart antennas [12], [11], FSO transceivers [14]) for more efficient medium usage and scalability. Previous work in directional antennas focused heavily on measuring network capacity and medium reuse [11]–[13]. In this paper, we utilize directionality for a novel purpose: to facilitate layer 3 routing without the need for flooding either in the route dissemination or discovery phase.

Our protocol, called Orthogonal Rendezvous Routing Protocol (ORRP) is based upon two simple ideas: 1) local directionality is sufficient to maintain forwarding of a packet on a straight line, and 2) two sets of orthogonal lines in a plane intersect with high probability even in sparse, bounded networks. ORRP assumes that each node has directional communication capability and can therefore have a *local sense of direction* (i.e., orientation of neighbors is known based on a local North). Notice that this is an even weaker form of information than a *global sense of direction* (i.e., orientation of neighbors is known based on a global North) which necessitates additional hardware such as a compass. Fig. 2 illustrates an example operation of ORRP.

Consider a source node S that wishes to send packets to a destination node D . Both nodes S and D have their own local notions of orientation. Source S sends route discovery packets in four orthogonal directions and the destination D does likewise for route dissemination packets. The route discovery packets will rendezvous at a node touched by a route dissemination packet at up to two rendezvous points on the plane. We refer to the intersection that facilitates a shorter path as the rendezvous node R . Node R directs packets from source S to the destination D . Node D 's state is only maintained on

Manuscript received August 22, 2006; revised June 20, 2007; approved by IEEE/ACM TRANSACTIONS ON NETWORKING Editor M. Buddhikot. First published July 15, 2008; current version published April 15, 2009. This work is based upon work supported by the National Science Foundation under Grant IGERT 0333314, Grant ITR 0313095, Grant STI 0230787, Grant 0721542, and Grant 0627039. Any opinions, findings, and conclusions or recommendations expressed in this material are those of the author(s) and do not necessarily reflect the views of the National Science Foundation. The work was done while authors were at Rensselaer Polytechnic Institute, Troy, NY 12180 USA. A preliminary version of this paper appeared in ICNP 2006, Santa Barbara, CA.

B. Cheng was with Rensselaer Polytechnic Institute, Troy, NY 12180 USA. He is now with the MIT Lincoln Laboratory, Lexington, MA 02420 USA.

M. Yuksel was with Rensselaer Polytechnic Institute, Troy, NY 12180 USA. He is now with the Computer Science and Engineering Department, University of Nevada at Reno, Reno, NV 89557 USA.

S. Kalyanaraman was with Rensselaer Polytechnic Institute, Troy, NY 12180 USA. He is now with the IBM India Research Laboratory, Bangalore 560071, India.

Digital Object Identifier 10.1109/TNET.2008.926511

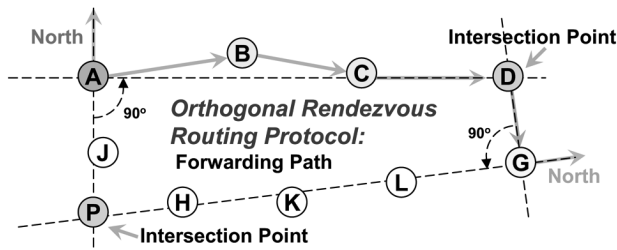


Fig. 2. ORRP basic example: Source sends packets to Rendezvous node which in turn forwards to Destination.

the two orthogonal lines, which implies that the total state complexity is $O(N^{3/2})$ for a network of N nodes. If each node chooses its local orthogonal directions independently, ORRP state information is fairly evenly distributed throughout the topology resulting in no single point of failure. Further, there is no flooding by either source S or destination D . All these factors enable scalability without imposing the requirement of an explicit hierarchical structure [4], [10]. In other words, ORRP offers a scalable, *unstructured* indirection method for routing in contrast to the hierarchically structured methods suggested in prior work. However, the ORRP paths chosen are suboptimal, i.e., have a stretch factor greater than 1 compared to the corresponding shortest paths. However, we show that this factor is not too large on average.

The rest of the paper is organized as follows. We first outline key design issues of ORRP in the next subsection. Section II deals with the specifics of ORRP including assumptions, concepts and examples. Section III provides performance analysis including basic Matlab simulations to formulate upper bounds on reachability and average shortest path while Section IV examines these issues in more realistic packetized simulation environments. Finally, Section V overviews related work and builds the context for ORRP while VI presents some thoughts on future work and concludes the paper.

A. Key Design Considerations

To fully realize the implications of ORRP, it is important to understand what issues traditional geographic routing protocols face. The problem of end-to-end wireless geographic routing using network localization can be broadly categorized into three layers as shown in Fig. 1. The lowest layer L1 is the localization scheme that obtains node coordinates [4], [2] while the second layer L2 maps these coordinates to node “identifiers” like a name or a number. Once these two are established, the third layer L3 uses this information to perform geographic routing. Current research in geographic routing protocols (e.g., GPSR [3], TBF [5], GLS [4], Landmark [18]) often tackle one of the three layers and assume the others to be a given. When taken separately, schemes in each layer can be shown to be extremely scalable. However, combining the effects of maintenance of the three layers can be rather costly. ORRP provides a simple, lightweight alternative to tackle layers L2 and L3 while removing the need for layer L1 altogether.

Specifically, ORRP focuses on and attempts to optimize based on the following considerations:

- *Connectivity Under Less/Relaxed Information*—Protocols such as GPSR [3] or TBF [5] operate under the assumption that each node has a globally consistent view of its own as well as other’s geographic positions. ID-to-location mappings (location discovery problem) are assumed to be a given. While this assumption is appropriate given the lowering cost of GPS receivers and several proposed methods of solving the location discovery issue [16], [17], maintaining global view of the network in this way can be costly, unavailable (e.g., GPS receivers need “sky access” and cannot be used indoors) and might not be scalable in larger or highly dynamic networks. ORRP eliminates the need for location discovery by utilizing the fact that two pairs of orthogonal lines mostly have intersection points. These “rendezvous points” act as forwarders of data increasing scalability.
- *Efficient Medium Reuse*—Topology-based routing protocols often fall into two camps: proactive (e.g., DSDV [7]) and reactive (e.g., DSR [9], AODV [8]). Proactive protocols consistently flood the network with control packets to maintain up-to-date routing tables at each node. While this ensures high packet delivery success even in mobile environments, scalability is limited due to the sheer number of control packets needed to maintain up-to-date routing tables. Reactive protocols attempt to solve this issue by requesting routes “on demand” and then caching those routes. While this works for less mobile environments, similar issues with scalability arise. ORRP mitigates these issues by forwarding control packets proactively only in orthogonal directions thereby freeing the medium for data, and then reactively requesting routes when one is not cached and is needed. These route requests do not flood the network unnecessarily because they are transmitted only in orthogonal directions and once a rendezvous node receives these request packets, it stops the forwarding.
- *Less State Information Needed to be Maintained*—Because ORRP only maintains routing information in orthogonal directions, scalability is increased.

In order to optimize and bring out the advantages listed above, there are several tradeoffs associated with ORRP:

- *Increased Path Stretch*—ORRP optimizes connectivity and efficient medium reuse with little agreed-upon information. The cost of less information is that packets often take paths longer than shortest path. We will show that although ORRP paths are suboptimal, under normal circumstances, the average path stretch is close to optimal.
- *Limited Reachability*—Due to possibility of no intersection of orthogonal lines, some source and destination pairs might not have rendezvous points resulting in unavailable paths. While several corrective measures are suggested in ORRP, we will show that under normal operation, the packet delivery success is extremely high.

II. ORTHOGONAL RENDEZVOUS ROUTING PROTOCOL

In this section, we will detail the assumptions, specifications, and mathematical aspects of ORRP. Specifically, we will 1) address assumptions made by ORRP including hardware requirements and other cross-layer abstractions; 2) detail the proactive

and reactive elements of ORRP; and 3) explain path deviation correction and void traversal with the Multiplier Angle Method (MAM).

A. Assumptions

ORRP relaxes many of the assumptions made by position-based routing protocols while still providing high connectivity. ORRP makes no assumptions on location discovery and uses packets forwarded in orthogonal directions to find paths to the destination from a given source. To do so, ORRP makes three major assumptions:

- *Neighbor Discovery*—We assume that any given node will know (i) its 1-hop neighbors and (ii) the given direction/interface to send packets to reach this neighbor.
- *Local Sense of Direction*—Each node must have its own local perception of direction (i.e., each antenna/transceiver knows its own orientation with respect to the “local north”).
- *Ability to Transmit/Receive Directionally*—Nodes must be capable of communicating directionally over their transceivers. This can be done by various hardware including directional and smart antennas [11], and FSO transceivers [14]. FSO transceivers are a particular interest due to their fine-grained transmit angle and ability for several dozen to be tessellated together oriented in several directions on a single node [14].

B. Theory

The basic concept behind ORRP is simple: knowing that in 2-D Euclidian space, a pair of orthogonal lines centered at different points will intersect at two points at minimum, rendezvous points can be formed to forward packets as shown in Fig. 2. To achieve this, ORRP relies on both a proactive element which makes up the “rendezvous-to-destination” path and a reactive element which builds a “source-to-rendezvous” route on demand. Nodes periodically send ORRP announcement packets in orthogonal directions and at each node along the orthogonal route, the node stores the route to the source of the ORRP announcement and the node it received the announcement from (previous hop). When a source node wishes to send to some destination node that it does not know the path for, it sends out a route request packet (RREQ) in its orthogonal directions and each subsequent node forwards in the opposite direction from which it receives the packet. Once a node containing a path toward the destination receives an RREQ, it sends a route reply packet (RREP) in the reverse direction back to the sender and data transmission begins. In the following subsections, we will detail and explain the tradeoffs associated with each element of ORRP.

1) *Proactive Element*: In order for a source and destination to agree upon a rendezvous node, pre-established routes from the rendezvous node to the destination must be in place. Because each node has merely a local sense of direction, making no assumption on position and orientation of other nodes in the network, it can only make forwarding decisions based on its own neighbor list. After a set interval, each node sends ORRP announcement packets to its neighbors in orthogonal directions as shown in Fig. 3. When those neighbors receive these ORRP announcement packets, it includes the source, previous hop, and

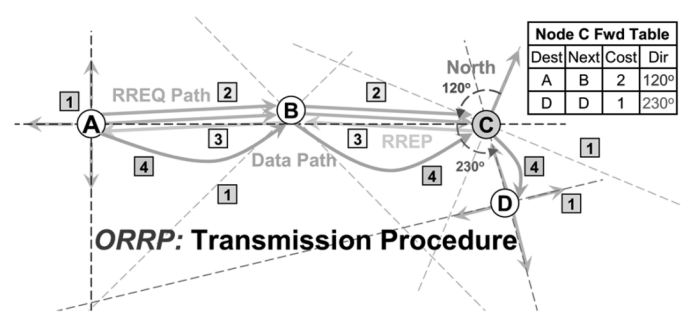


Fig. 3. 1: ORRP Announcements used to generate rendezvous node-to-destination paths. 2-3: ORRP RREQ and RREP packets to generate source-to-rendezvous node paths. 4: Data path after route generation.

hop count into its routing table as a “destination-next-hop pair” and forwards it out the interface exactly opposite in direction from the interface it received the packet. Although we currently only consider hop-count to be the metric for path selection, it is easy to adapt ORRP to use other heuristics such as ETX [21] among others.

It is important to note that each node does *not* maintain a complete picture of the network which limits the state information needed to be updated, and thereby increasing scalability. Moreover, only forwarding in orthogonal directions provides enhanced medium reuse. Based on mobility speeds, energy constraints, and other factors, parameters that can be tweaked for higher performance of ORRP announcements include *announcement send interval* and *forwarding entry expiry time*. Because the forwarding table only maintains information about destination and next hop, overhead in storage and maintenance is minimized as well.

2) *Reactive Element*: In order to build the path from source to rendezvous node, an on-demand, reactive element to ORRP is necessary. When a node wishes to send packets to a destination that is not known in its forwarding table, it sends out a route request packet (RREQ) in all four of its orthogonal directions. When neighbor nodes receive this RREQ packet, it adds the reverse route to the source into its routing table and forwards in the opposite direction.

In a 2-D Euclidian plane, by sending a RREQ packet in all four of its orthogonal directions, it is highly likely to encounter a node that has a path to the destination. When a node with a path to the destination receives the RREQ, it sends a RREP packet back the way the RREQ came. Because each node along the path stored a reverse route to the source, it is able to forward the RREP back efficiently after recording the “next-hop” to send to this particular destination. When the source receives the RREP, it generates a “destination-next-hop” routing entry and forwards packets accordingly.

Fig. 3 illustrates the process of sending RREQ and RREP packets while showing the ORRP path selected. Unlike AODV, DSR or other reactive protocols, RREQ packets are *not* forwarded until they reach the destination, but only until it intersects a rendezvous node. The proactive element of ORRP takes care of the rendezvous node-to-destination path.

It is important to note that ORRP path is *not* equivalent to the shortest path for most cases. As mentioned earlier, we gained

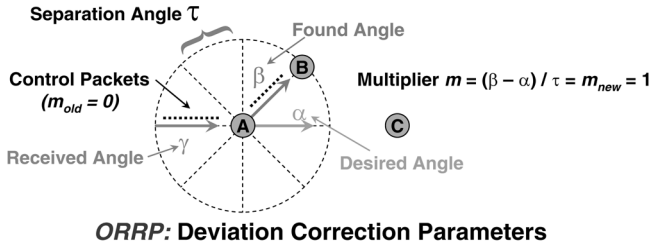


Fig. 4. ORRP multiplier angle method parameter illustration.

connectivity under relaxed assumptions at the cost of sub-optimal path selection (increased path stretch). We will show later, however, that the path selection is close to optimal, resulting in a fairly nonexistent cost.

3) *Deviation Correction: Multiplier Angle Method*: Up until now, we have considered only situations where nodes forward in orthogonal directions assuming that neighbors are all aligned on a straight line. In reality, however, straight line paths in random networks rarely exist. Although ORRP works on *path intersections* and as a result, does not need to enforce the rule that packets sent in orthogonal directions must remain true to their path, upholding this rule increases the probability of finding intersections. Ref. [15] shows that two straight lines randomly drawn in a euclidian plane have a 69% chance of intersecting within a given area. We will show in later sections that *two* pairs of orthogonal lines have a 98% chance of intersecting.

To address the deviation issue, it is important to clarify a few key concepts and limitations. First, deviation corrections can only be done when the deviation is greater than the conical spread of the directional antenna or transceiver. Interfaces oriented in a circular fashion, so that each of the antennas attached to a particular node operate at a set angle from the local “north”, have a coverage much like a pizza pie. Depending on the beam width and assuming no overlap in spread, a node can be at various degrees of deviation from the actual orientation of each particular antenna even though it is within the beam spread/coverage area. ORRP does *not* deal with deviations that occur *within* one antenna coverage area.

Next, ORRP assumes that the relative distances from one hop to another are relatively equal. In dense networks, this is a safe assumption due to the sheer volume of nodes. It will be shown that sparse networks do not care about distances either way due to lack of nodes. Finally, all deviation corrections are done at the RREQ and ORRP announcement level so that data transmission does no such calculations per hop.

ORRP addresses the issue of deviation correction by a *multiplier angle method (MAM)*. Each RREQ and ORRP announcement packet has an additional field in the packet header: deviation multiplier. For simplicity, we assume that all nodes have equal number of transceivers each separated with equal distances. The deviation multiplier is used to calculate the deviation angle from the desired angle at which a packet was sent. Table I defines a few key parameters which are illustrated in Fig. 4.

When searching for a next-hop within the corresponding antenna/transceiver beam width, ORRP cycles through all its

TABLE I
MULTIPLIER ANGLE METHOD DEFINITIONS

Received Angle (γ)	The angle node received packets from.
Deviation Angle (θ)	The angle to add/subtract in order to correct the deviation.
Desired Angle (α)	The desired angle to send out.
Found Angle (β)	The angle of transceiver found closest to desired angle with neighbor nodes.
Separation Angle (τ)	The angle of separation between each transceiver.
Multiplier (m)	The value to multiply τ by to find new desired angle.

neighbors and finds one which requires an antenna-deviation angle yet is still confined to less than $\pm 45^\circ$ (if packet is at originator) or $\pm 90^\circ$ (if packet is merely a forwarder) of the original direction. If a packet is at the originator, only $\pm 45^\circ$ needs to be searched because each of the four orthogonal directions is sending. So, giving each direction a 90° coverage effectively covers all directions. In the forwarding case, however, because only one direction is considered with potentially “void” spots, a greater angle range is given to traverse “voids” yet ensure packets are not forwarded directly the opposite direction. If no neighbor is found satisfying these conditions, the packet is dropped and an error is flagged. The following equations are used to calculate angle to send and what state to store in each packet (all angle values are between 0° and 360°):

$$\text{DevAngle } \theta = \min \left(+\frac{\pi}{2}, 2 * (\tau * m) \right), m \text{ positive} \quad (1)$$

$$\text{DevAngle } \theta = \max \left(-\frac{\pi}{2}, 2 * (\tau * m) \right), m \text{ negative} \quad (2)$$

$$\text{Desired Angle } \alpha = \gamma + \pi - \theta \quad (3)$$

$$\text{Multiplier } m = \frac{(\beta - \alpha)}{\tau} \quad (4)$$

At each hop, the node unpacks the multiplier from the packet header and calculates a desired angle to send out based on (3). It then searches through its neighbors which have corresponding transceiver angles and finds one with the closest angle to the desired angle. When one is found, a new multiplier is calculated based on (4) and stored into the forwarding packet header before the packet is sent out. The process is repeated until the packet arrives at the destination. Algorithm 1 breaks down the process step-by-step.

Algorithm 1 Multiplier Angle Method

- 1: Unpack old multiplier m
 - 2: Calculate angle needed to correct deviation θ (From (1) and (2))
 - 3: Calculate desired angle α (3)
 - 4: Find interface with direction closest to α that has a neighbor (found angle β)
 - 5: Calculate new multiplier m (4)
-

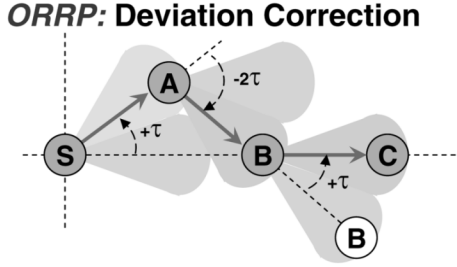


Fig. 5. Basic deviation correction example with Multiplier Angle Method.

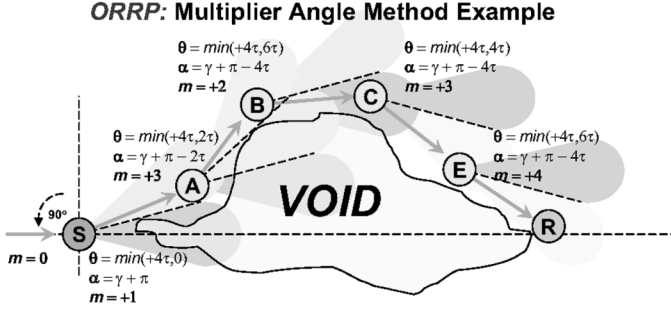


Fig. 6. Multiplier angle method to traverse voids in sparse networks while maintaining direction.

An example of our proposed *multiplier angle method* for deviation correction is shown in Fig. 5. Node S is sending packets along the line. Because it has no nodes along the line in range of its transceivers, S opts to send to node A which is at a transceiver angle of τ from the desired angle α and encode multiplier m of one into the packet header. When node A receives S's packet, it calculates the desired outgoing interface based on (3) and as a result, sends to Node B while encoding a multiplier m of zero because there is no deviation from desired angle and found angle. The rest is self-explanatory.

Potential problems may arise if the problem is cascading: Suppose node A wishes to send in the correct direction but has no neighbors in that direction. So, we continue with the original method of choosing a neighbor closest to the deviation angle and sending it. However, ORRP still maintains the multiplier angle method and corrects large deviations with larger forwarding angles. In dense networks, there should be no issues obtaining proper nodes to forward in a straight line.

C. Discussion

In this subsection, we will see how ORRP deals with sparse networks and corner routing in addition to examining protocol implications, potential issues, and future considerations.

1) *Sparse Networks*: Although the concept of ORRP centers around sending packets in four orthogonal directions, it easily adapts to sparse network cases as ORRP merely seeks for rendezvous points between source and destination probe packets. ORRP works based on the assumption that source's and destination's "probe packets" will eventually intersect at a point. That intersection point, however, need not necessarily be along the orthogonal paths. If in the process of sending out RREQ packets, a path is navigated in a curve-like fashion (as opposed to a straight line) due to lack of nodes, which intersects with a

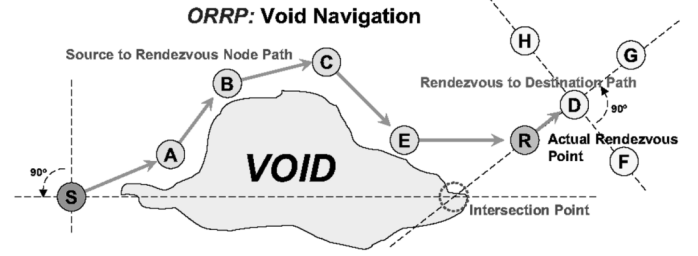


Fig. 7. Traversing voids in sparse networks with differing intersection points.

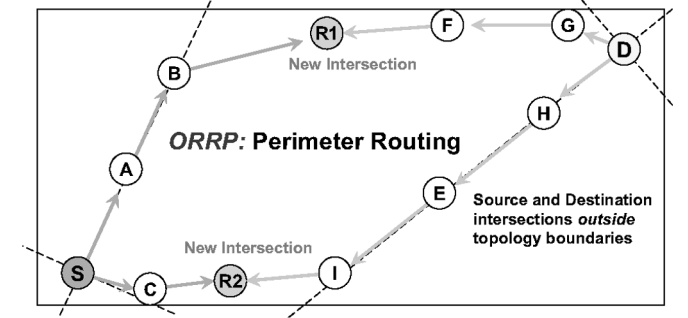


Fig. 8. Forwarding along perimeter is using MAM deals with corner cases where node intersections are outside of topology boundary. Appropriate TTL for ORRP announcement and RREQ packets must be set to minimize excessive state.

node that knows the path to the destination, then a path from source to rendezvous node to destination can easily be built.

Fig. 6 illustrates using ORRP's *multiplier angle method* of deviation calculation to navigate around an area devoid of nodes (only one direction is shown). Assuming that node R contains a path to S's intended destination, S's RREQ packets can traverse the perimeter of the void until it reaches node R. Calculations for each step of the way are shown and derived according to (1)–(4). Fig. 7 shows a complete path selection from source to destination given a sparse network and no nodes at intersection points.

The multiplier angle method (MAM) differs from GPSR's perimeter routing and many other face routing techniques in several ways. Firstly, because ORRP seeks only intersections with rendezvous nodes that contain a path to the destination, it is not trying to reach a specific node (assuming that rendezvous nodes will successfully deliver to destination). This allows for much higher flexibility and less stringent requirements for path selection. Secondly, MAM is an inherent nature of ORRP and *not* a special case that switches on and off like GPSR's perimeter routing. Additionally, GPSR's packets maintain additional states such as the node it entered the perimeter routing, points on the coordinate space, and destination information whereas ORRP's MAM requires only one state updated at each node resulting in reduction in overall space. MAM, therefore, offers a much more unstructured and lighter alternative to GPSR's perimeter routing.

2) *Perimeter Nodes*: Our analysis in Section III shows that "corner nodes" have a much higher probability of having no intersection points within the network topology with purely straight line paths. The multiplier angle method allows for state information to be propagated along the network perimeter as long as its send angle is within $\pm \frac{\pi}{2}$ of the desired direction.

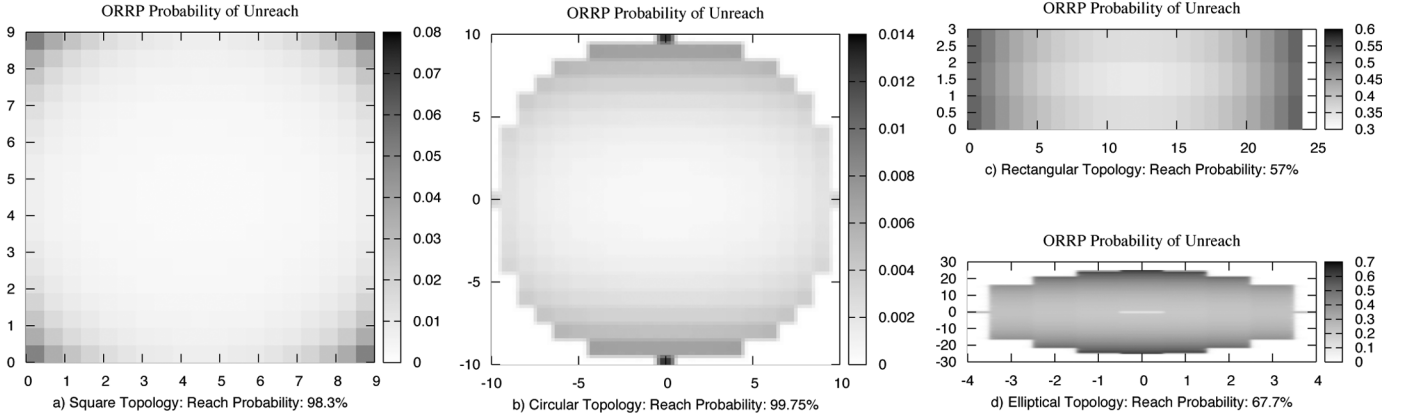


Fig. 9. ORRP reachability for various topology areas: Nodes in darker regions are less reachable. The strength of the darkness of a point shows the probability that a node located on that point will be unreachable by any other node on the area. It can be seen that topology corners and edges suffer from the highest probability of unreach.

Fig. 8 shows the problem as well as how MAM mitigates the issue. While this prevents packets from traversing back on itself, it is important to set a TTL on ORRP control packets to ensure that perimeter nodes do not get saturated with state information. Section IV describes simulation results on TTL's affect on reachability, path length, and state maintenance.

3) *MAC Layer Issues*: Choudhury *et al.* [33] bring up several concerns with the nature of directional antennas' asymmetric gain resulting in collisions and hidden terminal problems. The main result shows that straight line routes are inefficient because of higher interference in the direction of ongoing communications. Sekido *et al.* [34] propose several MAC level solutions to the problem without taking obscure paths to avoid hidden terminal problems and because ORRP focuses more on the routing layer, we do not feel these MAC layer issues are a problem.

III. ANALYSIS

As mentioned in the introduction, ORRP provides connectivity with less information at the cost of suboptimal path selection. In this section, we will examine metrics of *reachability* and *average state complexity* with network growth under a set of conditions and topologies while also observing *path stretch* to determine how much inefficiency in path selection we are trading off to utilize ORRP. Note that for all numerical analysis, our model does *not* consider details such as angle deviation correction and whether a rendezvous node at the particular point exists. Specifically, we will attempt to characterize bounds on how varying topologies affect reachability, state complexity, and path stretch in the base case.

A. Reachability Upper Bound Analysis

For our numerical analysis, given a Euclidian area over which nodes are scattered, a source–destination is said to be unreachable if all rendezvous points are outside the boundaries of the topology area. In order to determine the reachability upper bound in this case, it is important to isolate cases where ORRP will fail based on source and destination location and orientation. Assuming a Euclidean 2-D rectangular topology with

$0 < y < b$ and $0 < x < a$ with nodes randomly oriented with “north” between 0° and 90° , we claim that an upper bound in packet delivery success utilizing ORRP is 99.4%.

The general idea behind obtaining the reachability upper bound is to find intersections between orthogonal lines between the source and destination. In cases where all the intersections lie outside of the rectangular area for a particular source and destination oriented in a certain way, ORRP fails to find a path. Notice that this analysis assumes that ORRP probe packets do not travel along perimeters of the Euclidian area under consideration and therefore inspects a worst case upper bound on reachability. In actual simulation implementation, we use very simple techniques (see Sections II-B3 and II-C2) to achieve 100% reachability in ORRP.

Our analysis begins with randomly selecting two source and destination pairs along with random orientations. We then formulate the equations of the orthogonal lines generated by these two nodes and randomly selected orientations and find their intersection points. If at least one of these intersection points lies in the boundaries of the topology, then we consider that particular source–destination pair as reachable. By iterating through all possible orientations for each possible source–destination pair, we find a percentage of the total combinations that provide reachability versus the total paths chosen. Because different Euclidian-area shapes will no doubt yield different reachability requirements, we calculated the reachability probability for various area shapes by using Matlab. We refer the reader to the Appendix for a detailed description of our reachability analysis.

Fig. 9 shows the varying degree of reachability depending on the topology shape. As can be seen, topologies that spread nodes in single direction such as a rectangle or ellipse with one of the sides much greater than the other yield poor results for reachability due to the fact that ORRP intersections often fall outside of the topology area more easily under those situations. While at first this seems rather disappointing, it is important to note that random topologies rarely fall into a rectangle with one side much longer than the other and even so, ORRP's MAM enables rough forwarding along perimeters to find intersection points, significantly enhancing reach.

TABLE II
COMPARISON OF AVERAGE STATE INFORMATION

	GPSR	DSDV	XYLS	ORRP
Node State	O(1)	O(n^2)	O($n^{3/2}$)	O($n^{3/2}$)
Reachability	High	High	100%	High (99%)
Name Res.	O($n \log n$)	O(1)	O(1)	O(1)
Invariants	Geography	None	Global Comp.	Local Comp.

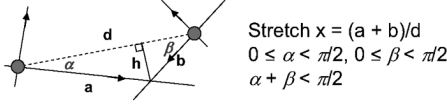


Fig. 10. Average stretch (ORRP path/shortest path) between two nodes.

B. State Information Maintained at Each Node

One of the major hindrances to network scalability is the amount of state information each node is required to maintain. In completely proactive routing protocols, nodes trade routing tables and other information on a regular basis to keep routes up to date. While this helps maintain connectivity even in highly mobile environments, maintaining such a vast amount of state information at each node requires extensive coordination and information transfer resulting in networks that scale poorly. Because ORRP only forwards routing announcements in orthogonal directions and only nodes along those lines maintain state information about the node sending announcements, it is expected that ORRP will incur less overhead in state maintenance.

We ran Matlab simulations for a square topology of nodes and calculated the total amount of state information each node maintained with respect to the total number of nodes in the system. Because the granularity in our simulation was one, we were able to calculate the total amount of state information maintained by iterating through each possible node and orientation combination and taking the average of the distance of the orthogonal lines to the borders of the topologies. This was used to calculate average total state maintained at each node. Our results showed that with rectangular and circular topologies, state scales on the order of $N^{3/2}$ with N being the number of nodes.

Table II shows the ORRP's state information maintenance compared to other protocols. Compared to GPSR with location mapping factored in, ORRP requires more state information to be maintained at each node but requires much less structure and global information to be shared. Looking at the opposite extreme, DSDV provides full connectivity and optimal path selection at the cost of a scalability. In comparison to XYLS [22], ORRP requires less information (local compass versus global compass) while achieving virtually similar reach.

C. Average Path Stretch

Because ORRP trades off suboptimal paths for connectivity under less information, it is important to see what conditions lead to unacceptable path choices and how much sub-optimality we are trading off for connectivity in an unstructured manner. We begin first by attempting to analyze and understand what kind of stretch values we should expect and then move onto Matlab and NS2 [19] simulations for more realistic values.

Suppose two nodes are trying to communicate with each other using ORRP as shown in Fig. 10 where d is the path length between the two points and a and b are the lengths of the two piece ORRP Path (source-to-rendezvous node and rendezvous node-to-destination). Because there can theoretically be two interception points between the pair of orthogonal lines resonating from the two nodes, path selection is based on the shorter of the two paths. The conditions listed in Fig. 10 bound the selection to the minimum ORRP Path. Stretch is defined as the ratio between the path selected (in this case, $a + b$) and the shortest path (d). Due to the nature of orthogonal lines, α and β are between 0 and $\pi/2$ and because there is an equal probability for each node to be oriented in a certain manner, α and β are uniformly distributed.

$$h = b \sin \beta = a \sin \alpha \quad (5)$$

$$d = b \cos \beta + a \cos \alpha \quad (6)$$

$$x = \frac{a + b}{d} = \frac{\sin \alpha + \sin \beta}{\sin(\alpha + \beta)} \quad (7)$$

Equations (5) and (6) come from basic trigonometry. Equation (7) represents the stretch x in terms of two uniformly distributed angles α and β . We know that the *probability density function* (PDF) of a random variable that is uniformly distributed is merely the inverse of the interval. The result is the *PDF* of α and β to be $\frac{1}{\pi/2}$ and $\frac{1}{(\pi/2)-\alpha}$ respectively, to satisfy the conditions listed in Fig. 10. The minimum stretch possible is merely the shortest path and therefore, one. The maximum stretch occurs when both α and β are at $\pi/4$ and $x = \sqrt{2} = 1.414$. As a result we expect the mean of the stretch to be somewhere between 1 and 1.414.

$$E[X] = \int_0^{\pi/2} \int_0^{\pi/2-\alpha} \frac{\sin \alpha + \sin \beta}{\sin(\alpha + \beta)} \left(\frac{1}{\frac{\pi}{2} - \alpha} \right) \left(\frac{1}{\frac{\pi}{2}} \right) d\beta d\alpha \quad (8)$$

$$E[X] = 1.125.$$

Equation (8) gives the expected value of the random variable X with respect to the two uniformly distributed angles α and β . Integrating the values over the chosen intervals yields a mean of 1.125 for the ORRP path stretch in *unbounded regions* (12.5% path stretch). Although not quite exactly shortest path, we can see that the stretch is still very low and in most cases, acceptable. Similar analysis leads to a variance of 0.0106 and therefore we can expect most of the path selections to be relatively close to shortest path.

Using Matlab, we created several bounded areas of various shapes and iterated through every possible source-destination pair in a "grid-like" way, along with every possible orientation for each node. We then built paths (distances) from the source to rendezvous node to destination and compared with the shortest path. If no rendezvous nodes were found within the boundaries of the topology, a path length of the perimeter of the topology was used in calculations, as this is the worst possible path length if packets are routed along perimeter. Fig. 12 gives the distribution of average stretch values for a square topology. As shown, the stretch values are confined between 1 and 1.414 and lean toward 1 as suggested by our calculated mean and variance.

Fig. 11 shows evaluated topologies along with ORRP path to shortest path ratios for nodes in each region. As expected, the rectangular topology yielded the highest path discrepancy with an average path stretch of 3.24. This is most likely due to the

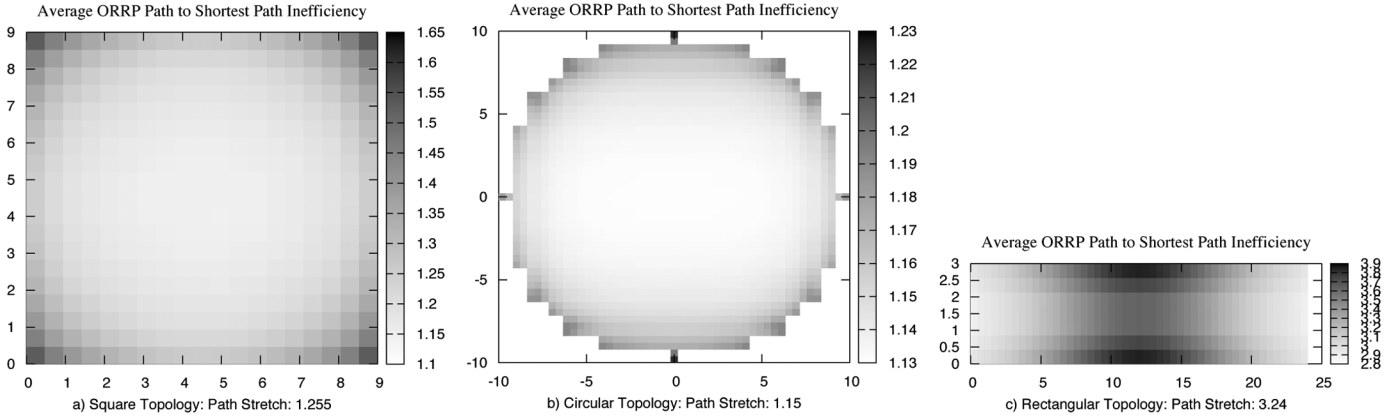


Fig. 11. ORRP Path versus Shortest Path Ratio: A node in darker regions have higher likelihood of having longer paths to a destination on the area. Topology corners and edges suffer from the higher stretch in symmetric topologies.

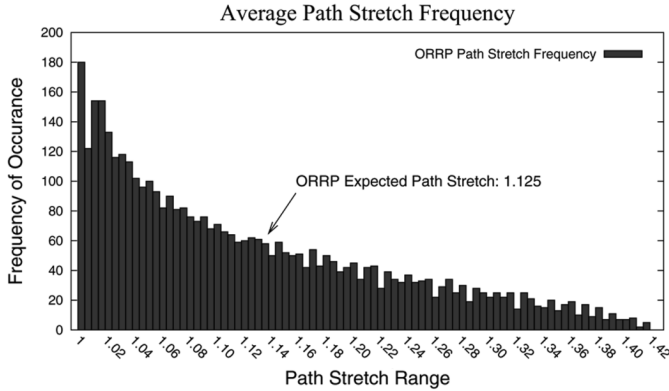


Fig. 12. Average stretch (frequency distribution of ORRP path stretch in square topology network). The stretch values are between 1 and 1.414 and lean toward 1 as suggested by our calculated mean and variance.

TABLE III
COMPARISON OF REACH PROBABILITY VERSUS NUMBER OF LINES

	1 Line (180°)	2 Lines (90°)	3 Lines (60°)
Circle (Radius 10m)	58.33%	99.75%	100%
Square (10mx10m)	56.51%	98.30%	99.99%
Rectangle (25mx4m)	34.55%	57%	67.61%

TABLE IV
COMPARISON OF PATH STRETCH VERSUS NUMBER OF LINES

	1 Line (180°)	2 Lines (90°)	3 Lines (60°)
Circle (Radius 10m)	3.854	1.15	1.031
Square (10mx10m)	4.004	1.255	1.039
Rectangle (25mx4m)	4.73	3.24	1.906
Grid (No bounds)	1.323	1.125	1.050

fact that in the reachability evaluations as shown in Fig. 9, the rectangular shape had the highest amount of unreachability resulting in the perimeter case needing to be invoked the most. The highest path discrepancy appeared in the middle of the rectangle due to the fact that nodes in the middle allow for the longest ORRP paths, reaching the left and right edges while the shortest path is extremely short (the middle to anywhere else directly is short). The results from the other topologies are also consistent with expectations in that the circular topology, with the greatest reach probability, yielded the smallest average path stretch.

D. Additional Lines Study

While our study focuses using a pair of orthogonal lines (one at the source and one at the destination) to build routing paths, it is interesting to see the effect of adding additional forwarding directions into the scheme. Specifically, we wish to see how the addition of lines affects reach probability, path stretch, and states maintained in the network. Our analysis was performed in Matlab with a grid network under varying topological boundaries without employing any deviation correction. For a step-by-step walk-through of the analysis method (for two lines), please see the Appendix.

Tables III and IV show the reachability and path stretch simulation results for 1–3 lines all equidistantly separated from each other. While for reach probability, the effect from one to two lines is dramatic, very little gain is achieved by adding additional lines. In the case of path stretch, however, the addition of additional directions to send announcement and RREQ packets result in much better path selection as more packet interceptions occur. We suspect that in sparser networks or networks with voids, the gains would be negligible as control packets would take similar paths with MAM. It is important to note that with MAM, almost all of the corner case reach issues can be resolved even with only two lines.

Fig. 13 demonstrates the potential increase in state maintenance needed with the addition of transmission lines. While increasing steadily, it is still much less than order N^2 .

IV. PACKETIZED SIMULATION AND EVALUATION

In this section, we will evaluate the metrics of *reachability*, *state maintenance*, *path stretch*, *end-to-end latency* and *aggregate network goodput* under conditions of varying *network densities*, *number of interfaces*, and *TTL values*. Unless otherwise noted, all simulations were performed using Network Simulator [19] with n interfaces (divisible by 4) and each interface having a beam-width of $360/n$ degrees. All simulations were averaged over two runs of five different randomly generated flat topologies (total 10 trials) and the 95% confidence intervals of the runs plotted. Our default simulation parameters are listed in Table V.

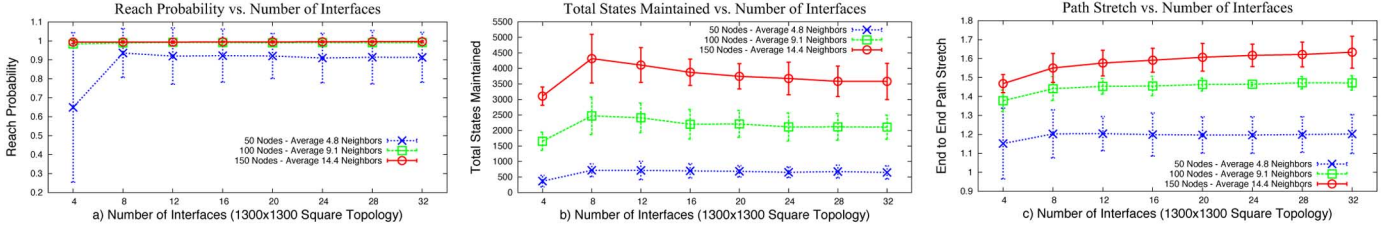


Fig. 14. ORRP reachability, total states maintained, and average path stretch versus number of interfaces for dense, average, and sparse networks. In sparse networks, increasing number of interfaces provides significant benefits at first but diminishing returns after 8 interfaces.

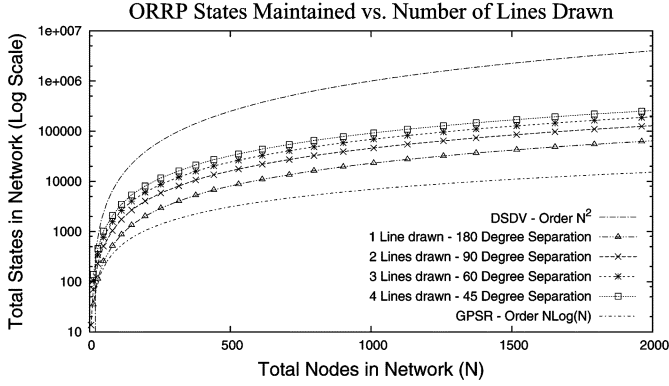


Fig. 13. Average stretch (total states maintained in network with respect to the number of transmission lines used). As number of lines increase, the number of states maintained throughout network increases.

TABLE V
ORRP DEFAULT SIMULATION PARAMETER

Parameter	Values
Transmission Radius	250.0m (NS2 Default)
TTL for RREQ/Announcement Pkts	10
Topology Boundaries	1300m \times 1300m - No Mobility
Queue Length	250
Announcement Interval	4.0s
Route Timeout	5.0s
Hello Interval	1.0s
Simulation Time	70s
CBR Packet Size / Send Rate	512 bytes / 2Kbps

A. Effect of Number of Interfaces on Varying Network Densities

One important consideration for nodes with multiple transceivers/antennas is to find a tradeoff between the number of interfaces versus performance gains. We speculate that by increasing the number of interfaces and thus increasing the granularity of angle calculations, reachability should increase simply because there are fewer neighbors assigned to reach interface. This allows for tighter control on next hop (instead of randomly choosing a next hop), increasing the odds of an announcement-RREQ “hit”. Furthermore, this tighter control on next hop should theoretically lead to better paths and lower end-to-end latency as well because straight lines are maintained more accurately. State should remain fairly fixed in each experiment because announcement intervals remain fixed across each run.

In this section, we will examine the tradeoffs in *reachability*, *state maintained per node*, and *average path stretch* in varying number of interfaces per node. Default parameters found in Table V were used, with each node in each run randomly

choosing transceiver orientations and a *local north*. Our first set of simulations focused on effect of number of interfaces and thus the transmission granularity, under three different sets of node densities (sparse with an average of 4.8 neighbors, medium with an average of 9.1 neighbors, and dense with an average of 14.4 neighbors). Our second set of simulations involved void traversals. It was expected that the more interfaces, the more effective the void traversals would be due to the more accurate calculations and availability of nodes.

Fig. 14(a) shows that in dense and medium networks, varying the number of interfaces had little to no effect on reachability as all nodes were reachable. As the network became sparser, however, we see a sharp increase from four to eight interfaces. We suspect that one of the major reasons for the increase in reach probability is the sheer number of nodes each transmission “cone” encompass. With fewer interfaces, each transmission “cone” needs to reach a lot more nodes than finer grained interfaces. This could result in packets being delivered orthogonally, but not necessarily intersecting due to poor node choice by the sender. Also, because four interfaces is not enough to perform adequate angle correction (even “correcting” a path by shifting by one interface essentially forwards packets 90° from the intended direction), announcement states are not adequately being seeded and RREQ packets often find it hard to keep moving “forward”. Up to a certain point, however, the granularity has less effect, especially in sparser networks.

Surprisingly, Fig. 14(b) also shows that there is a fairly large increase in total states maintained network-wide from four to eight interfaces and continues to decrease with increasing number of interfaces. As with the reachability, we believe that the increase in states from four to eight interfaces stems from a large change in ability to perform MAM angle correction. With only four interfaces, there is little to no angle correction because again, even shifting transmission by one interface essentially forwards packets 90° from the intended direction.

The reason why there is a slight *decrease* in states from 8–16 interfaces (and it is much more noticeable with denser networks), is because in the announcement phase, each node randomly chooses a neighbor in a set antenna/interface direction to send to. In cases where there are more than one neighbor associated with a specific interface direction (such as in denser networks), announcement packets at two different intervals sending out the same direction might potentially be sent to two different neighbors. There is, therefore, an increase in state maintained simply because the neighbor to first receive the announcement will have an entry for the state until it expires and the neighbor to receive it later will have also have an entry for the state. The result is consistent as the decrease in number

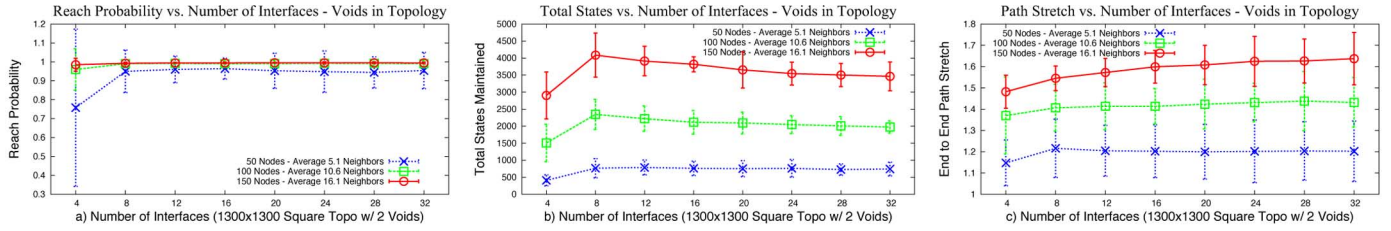


Fig. 15. ORRP reachability, total states maintained, and average path stretch versus number of interfaces for dense to sparse networks with large voids present. Small gains can be seen by adding more than 8 interfaces in all cases.

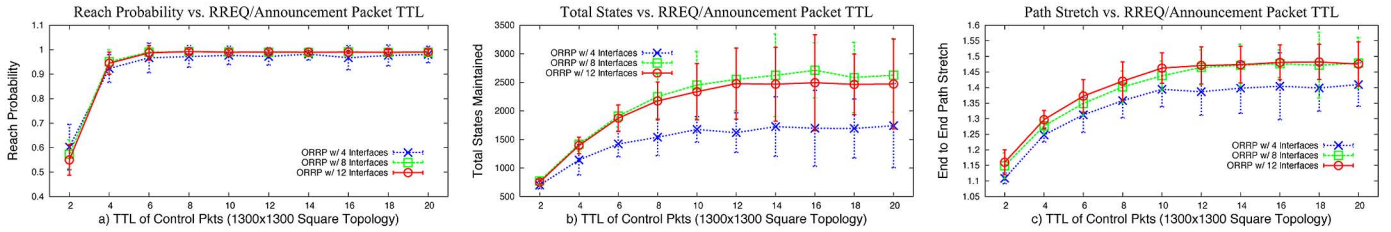


Fig. 16. ORRP reachability, total states maintained, and average path stretch versus control packet TTL for various number of interfaces. Increasing TTL up to a certain point does not effect reach probability, states maintained, and average path stretch.

of states maintained network-wide happens only when the average number of neighbors per node is close to or more than the number of interfaces. The total state is also consistent with our initial Matlab analysis, which showed that ORRP state scaled on order $N^{3/2}$ (roughly 650 states for 50 nodes, 2100 states for 100 nodes, and 3600 states for 150 nodes).

Our final metric was to examine average end-to-end path stretch as a function of the number of interfaces. Because ORRP has no notion of neighbor distances, it arbitrarily chooses a neighbor in the interface direction it wishes to send. At times, this neighbor could be one that is closer to the destination geographically or sometimes it could be farther. Therefore, it makes sense that with a denser network (more neighbor choices), the average path stretch will be higher (nodes might choose neighbors that are closer to itself and require more hops to destination).

Fig. 14(c) shows the difference mentioned above well for sparse to dense networks. With the increase in node density, path stretch increases as expected. Although it was expected that with an increase in number of interfaces, denser networks will no doubt decrease in path stretch due to finer granularity in selecting a next-hop neighbor to send, we were surprised to find that this was not the case. With increased network density, increasing the number of interfaces actually led to a slight increase in end-to-end path stretch. To reconcile this issue, we defer back to our explanation of the number of states maintained network-wide. With the fewer number of states maintained network-wide due to lessened “randomness” in choosing next-hop paths in a specific interface direction, rendezvous paths are more rigid resulting in longer paths chosen.

B. Effect of Number of Interfaces on Network Voids

Navigating through voids in our network topology results in higher reliance on the MAM of deviation correction. Because the MAM’s efficiency increases with a higher granularity of transmission interfaces (the more interfaces to choose from lead

to better ability to control path curves), we hypothesized that by increasing the number of interfaces, more efficient paths could be found resulting in higher reachability. The conditions for the simulations were consistent with Section IV-A with the only difference being that the topologies included two voids and had an average of 5.1, 10.6, and 16.1 neighbors per node for the sparse, average, and dense network cases, respectively. Fig. 15 shows our results.

Much like in Section IV-A, our results showed a noticeable increase in reachability with an increase of interfaces from four to eight in both the sparse and average network density case. Again, this is expected due to lack of angle correction options with only four interfaces and these results explain the large change from four to eight interfaces in the other figures as well. Total state information network-wide was seen to decrease from 8 to 32 interfaces due to lessened randomness in choosing next hop neighbors in a specific interface direction. As explained previously, having less interfaces meant that each interface “covered” more neighbors. When announcements are transmitted at set intervals, it randomly chooses a neighbor in the direction it wishes to transmit packets in and sends it to that neighbor. If an interface has multiple neighbors, state information is potentially propagated to both neighbors at different intervals. The overlapping period between when the first state expires at the first node and when the second state arrives at a new node is what causes the extra states network-wide. When there are fewer interfaces, this randomness and overlapping states is removed.

The state issue is also what causes increased path stretch as the number of interfaces increase. The more states are seeded network-wide, the more path choices are available. The only surprising difference in comparing the simulations with and without voids is that with voids, the average end-to-end latency difference in dense and sparse environments is much smaller. This is perhaps due to sparse networks not having many alternatives in path selection to traverse voids, resulting in similar path choices for various end to end paths.

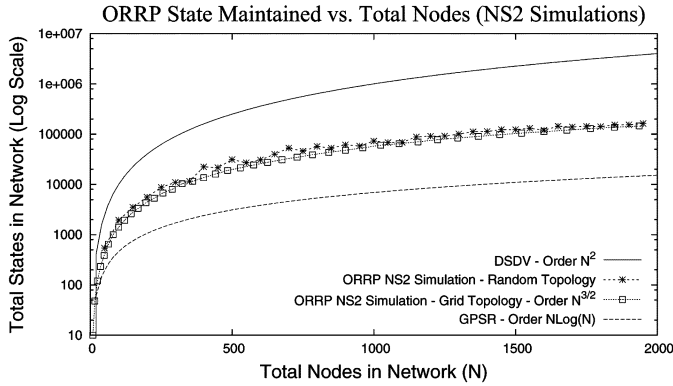


Fig. 17. NS2: ORRP total state maintained versus total nodes in network.

C. Effect of Control Packet TTL on Varying Network Densities

MAM attempts to minimize deviations in path. In sparse networks, however, announcement packets scheduled for orthogonal directions might initially be sent through the same path due to lack of neighbor options. In traditional routing announcements, one of these packets would be dropped to minimize overhead. In ORRP, however, there is a potential for the packets to “split” to different paths as neighbor density increases. ORRP limits a continual flood of announcement and RREQ packets through packet TTL. While in many cases, packet drops would occur at the network perimeter due to ORRP’s MAM forwarding conditions, TTL plays an important role in amount of state needed to be maintained at each node.

Fig. 16 shows the affect of TTL on the reachability, total states maintained, and average path stretch. Our results showed that varying the number of interfaces did not affect the outcome of the TTL study under average density conditions. We also ran extensive simulations on the effect of the number of interfaces had on each of the metrics under various network densities. Results from those simulations (which are beyond the scope of this paper) showed that under sparse network conditions, number of interfaces has a greater affect on the reachability, average states maintained, and path stretch.

Results from our TTL simulations show that as the TTL is increased, a steady increase in reachability and number of states maintained network-wide occurs and reaches a saturation point. This is to be expected because the network size and transmission range of the nodes dictate that almost all nodes should be able to be reached within 6–7 hops. Even for a TTL of 4 which should result in paths of eight hops (four hops from source to rendezvous node, four hops from rendezvous node to destination), much of the network (90%+) is reachable. Saturation is reached as the MAM takes over and prevents additional forwarding along the perimeter, which is consistent with our results.

D. State Information Maintained

ORRP was run in with grid and random topologies for several numbers of nodes and the total state maintained throughout the network tracked. Fig. 17 shows the total amount of states maintained versus the total number of nodes in both grid and random topologies. Lines fitted to both plots show an order $N^{3/2}$ maintenance of state at each node.

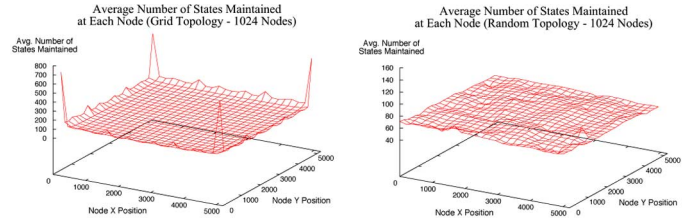


Fig. 18. NS2: State maintained in network topology. ORRP state is evenly distributed throughout the network.

To understand the distribution of where on the topology nodes generally kept more state, a 1024 node scenario was run in grid and random topologies and the amount of state kept at each node was averaged over 10 trials. Fig. 18 shows that edge nodes in both grid and random topologies maintained more state than usual. This is expected as perimeter nodes often bear the brunt of deviated routes. One interesting thing to note is that the amount of state information kept at each node is relatively consistent throughout the entire network. This finding is important because it shows that ORRP states are highly distributed and that no single point of failure will drastically affect the network.

E. Evaluation versus AODV, OLSR, and GPSR w/ GLS

In this subsection, we compare the packet delivery success ratio, aggregate network goodput, and average packet latency under ORRP, AODV, OLSR, and GPSR w/ GLS. CBR packets were sent from every node to every node in the network for 10 seconds at an increasing rate. Because ORRP takes advantage of directionality for medium reuse, it was expected that more packets would be delivered and a higher aggregate network goodput would result. Our results in Fig. 19 show that even with a very small rate of CBR packets, all-to-all connections flood the network and AODV, OLSR and GPSR w/ GLS are unable to deliver most of the packets sent.

In addition, ORRP is able to deliver a higher amount of data even with suboptimal paths due to the fact that it uses the medium more efficiently. It is important to note that goodput is very dependent on link load and as shown, the more loaded the network is, the lower the goodput. The average latency graph shows that initially, data sent using AODV, OLSR, or GPSR w/ GLS have very high latency. This is expected because even at a low rate, these protocols flood the network. Latency gets better with increased CBR because only successful packet transmissions are measured and with AODV, OLSR, and GPSR w/ GLS, very few packets are getting through. With ORRP, latency is initially very good because the network is not very saturated. As the network becomes more saturated, however, delivery latency increases.

V. RELATED WORK SURVEY

There has been a considerable amount of work on wireless routing protocols in recent years. Classified into five major types (reactive, proactive, hierarchical, position-based, and hybrid of the approaches), these protocols rely on different assumptions and tradeoff metrics like connectivity, path selection, overhead, etc., to route packets through a network.

Reactive protocols like AODV [8] and DSR [9] perform route discovery by flooding the network and delay data from being

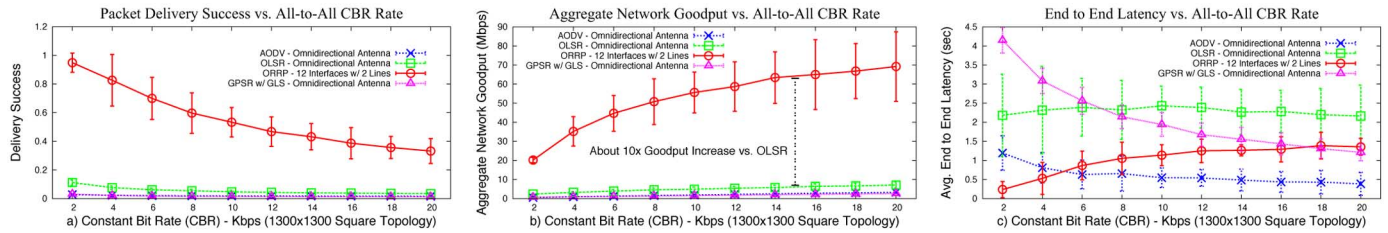


Fig. 19. Delivery success, aggregate network goodput, and avg. packet latency measurements for ORRP as compared to AODV, OLSR, and GPSR w/ GLS.

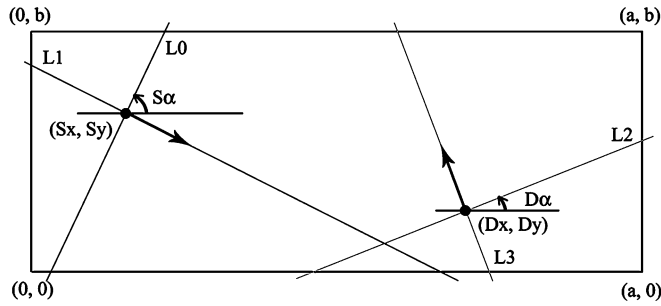


Fig. 20. ORRP unreachable probability calculation.

sent until a route is found. While considerably less state needs to be maintained at each node, route-discovery flooding of the entire network can be costly and inefficient. By contrast proactive protocols like DSDV [7] and OLSR [23] periodically broadcast routing information across the network (or in certain areas of the network), and maintain extensive routing tables at each node. Each data packet references the routing table of every hop in the packet and forwards accordingly. In much the same way as reactive protocols, heavy network floods of control packets incur high overhead and can be inefficient.

As a response to apparent issues with scalability of traditional reactive and proactive protocols, hierarchical and position-based approaches were examined heavily. Hierarchical routing protocols such as HRP [10], LANDMAR [18], and L+ [24] splice the network into regions that maintain routing information within the area. Certain nodes within each region are selected to be gateway nodes which maintain overlay routing tables with gateway nodes from other regions. Thus, routing within each region happens normally while routing inter-region is handled by the gateway node. While an important step in achieving greater scalability, hierarchical routing techniques rely too heavily on the special nodes that maintain routing between regions, and increased complexity of reorganization make it harder to implement.

Position-based protocols like GPSR [3] and TBF [5] tackle the issue of scalability by leveraging geographic position to route packets maintaining little to no state. A packet is forwarded in the “general direction” of the destination until it is reached. While highly scalable in a pure routing-only framework, position-based protocols assume location-to-address mapping techniques such as GLS [4], and node-localization equipment, such as GPS receivers, which incur additional overhead. Hybrid protocols like ZRP [26] and LGF [25] that combine the various strategies add benefits but still suffer from some form of flooding and capacity constraints.

In recent years, there has been a big shift from using structured schemes, such as GLS [4], which partitions networks into grids that trade location information on a limited basis, to unstructured schemes, such as DHT and virtual coordinate-based approaches [29], [28], [27]. DHT/virtual coordinate based approaches such as DPSR [28], VRR [27], among others, build hashes between node IDs and a set structural representation of the nodes. For example, DPSR [28] utilizes fingers that extend from a node while VRR [27] stores hashes in a circular format. These unstructured approaches not only effectively remove the need for a positioning system and network flooding, but also makes routing more scalable.

Braginsky *et al.* [15] proposed an unstructured rendezvous-abstraction routing technique based on drawing single lines. Events are broadcasted by nodes through random walks and event request packets are sent in a similar way until it intercepts event regions. It was shown that two lines bounded in a rectangle had a 69% chance of intersecting within the rectangle. By adding an additional line orthogonal to the original line, ORRP achieves much higher reachability (98.3% in areas where edges are almost equal) and robustness.

ORRP positions itself as an unstructured hybrid routing paradigm which uses directional transmission techniques to route packets based on rendezvous abstractions. Directional transmission techniques such as directional antennas and FSO transceivers have long been thought of as a possible means of augmenting current routing protocols to more effectively utilize the medium [30], [12], [13], [11], [14]. ORRP takes directionality a step forward by actually utilizing it in layer 3 routing. Instead of flooding the network with state maintenance packets like in many proactive routing protocols, ORRP sends announcement packets only in orthogonal directions, which allows the network to scale more effectively while, at the same time, builds rendezvous node-to-destination paths.

Similar to reactive protocols, ORRP sends out route-request packets in orthogonal directions to find a source-to-rendezvous node path. This is in contrast to reactive routing protocols, not only because it does not flood the network, but also because RREQ packets merely look for paths to the destination rather than the actual destination, cutting down on the amount of control packets that need to be sent. Unlike hierarchical approaches, ORRP does not place emphasis on specific nodes to have more state information, increasing robustness because there is no single point of failure.

Although several attempts have been made to deal with void and perimeter navigation [3], [31], all the attempts seek an end-to-end solution: mainly, paths are calculated based on

source and destination locations. ORRP differs from these methods in that it merely seeks for intersections with rendezvous nodes that contain a path to the destination rather than a complete source–destination solution. This fact relaxes the need for strict destination information and, when coupled with MAM to keep packet paths as “straight as possible”, provide an important alternative to face routing techniques proposed in [3] and [31].

VI. FUTURE WORK AND CONCLUSION

In this paper, we presented the Orthogonal Rendezvous Routing Protocol (ORRP), an unstructured forwarding paradigm based on directional communication methods and rendezvous abstractions. By taking the intersection of orthogonal lines originating from source and destination, packets from the source are forwarded to rendezvous nodes which in turn hand them over to the destination, providing simplified routing. We have shown that ORRP provides connectivity under lessened global information (close to 98% reachability in most general cases), utilizes the medium more efficiently (due to directionality of communications), and state-scales on order $N^{3/2}$ at the cost of roughly 1.12 times the shortest path length. In addition, simulations performed on random topologies show that state information is evenly distributed throughout the system, and, as a result, no single point of failure is evident.

ORRP’s benefits all stem from using lines to find intersection points between source and destination. Routing protocols that rely on localization schemes and/or flooding of the network with control packets often find themselves limited in scaling potential due to the amount of information needing to be disseminated throughout the network. ORRP provides highly scalable routing under relaxed and unstructured global information for wireless networks with directional communications support.

While we have only considered ORRP in the context of static wireless mesh networks, there are several directions for future work. Firstly, it would be interesting to investigate how ORRP fits into a context of a hybrid network network containing nodes with both directional antennas and omnidirectional antennas. Other area of consideration are mobility and how to prevent routing loops and provide error correction.

APPENDIX

In this Appendix, we outline our approach for calculating ORRP’s reachability probability for a rectangular topology area. Similar approaches were taken to obtain the results for circular and elliptical topologies shown in Fig. 9.

Given a Euclidean 2-D rectangular topology area defined by coordinate ranges $0 < y < b$ and $0 < x < a$, we assume that the nodes are randomly oriented with local “north” between 0° and 90° . Our goal is to find the probability that a randomly selected source–destination pair in this rectangular area will not be able to reach each other.

We first find the conditional probability that a particular source point will not be reachable by any other point in the area. Given a source located at (S_x, S_y) and oriented in S_α such that $S_\alpha \leq 90^\circ$, $S_x \leq a$ and $S_y \leq b$ (node is within the bounds of the topology), we assume that L_0 and L_1 are orthogonal lines that intersect source S with one line oriented in the direction S_α . Now, suppose that the source S wishes to

send to a destination node D located at $D = (D_x, D_y)$ with D_α such that $0 \leq D_\alpha \leq 90^\circ$, $D_x \leq a$, $D_y \leq b$ and L_2 and L_3 are orthogonal that intersect at D with one oriented in the direction D_α . We need to analytically construct the condition that the source S will be unreachable by any destination D . To do so:

Step 1: We formulate the slopes (m) and the equations for the four lines L_0, L_1, L_2 , and L_3 . As an example, for line L_0 , we formulate as follows:

$$\begin{aligned} L_0 : m_0 &= \tan(S_\alpha) \\ y_0(x) &= x \tan(S_\alpha) + S_y - \tan(S_\alpha) \times S_x. \end{aligned} \quad (9)$$

Step 2: We determine four possible intersection points (excluding the source point S and the destination point D) among the lines L_0, L_1, L_2 , and L_3 :

$$\begin{aligned} L_2 \text{ and } L_0 : (x_{20}, y_{20}) \text{ s.t. } y_0(x_{20}) &= y_2(x_{20}) \\ L_2 \text{ and } L_1 : (x_{21}, y_{21}) \text{ s.t. } y_1(x_{21}) &= y_2(x_{21}) \\ L_3 \text{ and } L_0 : (x_{30}, y_{30}) \text{ s.t. } y_0(x_{30}) &= y_3(x_{30}) \\ L_3 \text{ and } L_1 : (x_{31}, y_{31}) \text{ s.t. } y_1(x_{31}) &= y_3(x_{31}). \end{aligned}$$

Step 3: We finally formulate the analytical unreachability conditions as that all four of the intersection points must NOT be in the topology rectangular area. Thus, constraints for intersection points for unreachability can be written as

$$\text{NOT}(0 \leq x_{20} \leq a \text{ AND } 0 \leq y_{20} \leq b) \quad (10)$$

$$\text{NOT}(0 \leq x_{21} \leq a \text{ AND } 0 \leq y_{21} \leq b) \quad (11)$$

$$\text{NOT}(0 \leq x_{30} \leq a \text{ AND } 0 \leq y_{30} \leq b) \quad (12)$$

$$\text{NOT}(0 \leq x_{31} \leq a \text{ AND } 0 \leq y_{31} \leq b). \quad (13)$$

To numerically calculate unreachability probability, we first obtain the intersection point coordinates in terms of $S_x, S_y, S_\alpha, D_x, D_y$, and D_α by using the line equations in the intersection point equalities (e.g., in (9)). For example, x_{20} and y_{20} can be derived as follows:

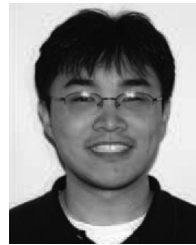
$$\begin{aligned} y_0(x_{20}) &= y_2(x_{20})x_{20} \tan(S_\alpha) + S_y - \tan(S_\alpha) \times S_x \\ &= x_{20} \tan(D_\alpha) + D_y - \tan(D_\alpha) \times D_x \\ x_{20} &= \frac{D_y - D_x \tan(D_\alpha) - S_y + S_x \tan(S_\alpha)}{\tan(S_\alpha) - \tan(D_\alpha)} \\ y_{20} &= \frac{D_y - D_x \tan(D_\alpha) - S_y + S_x \tan(S_\alpha)}{\tan(S_\alpha) - \tan(D_\alpha)} \\ &\quad \times \tan(S_\alpha) + S_y - S_x \tan(S_\alpha). \end{aligned} \quad (14)$$

Then, we calculate the intersection point coordinates for all possible values of S_x and D_x between 0 and a , S_y and D_y between 0 and b , and S_α and D_α between 0° and 90° , while checking the unreachability constraints (10)–(13). By running through all possibilities, we calculate the ratio of the number of S - D pairs satisfying the constraints and the total possible number of S - D pairs, which is the unreachability probability.

REFERENCES

- [1] B. Cheng, M. Yuksel, and S. Kalyanaraman, “Orthogonal rendezvous routing protocol for wireless mesh networks,” in *Proc. IEEE Int. Conf. Network Protocols (ICNP)*, Santa Barbara, CA, Nov. 2006, pp. 106–115.

- [2] S. Ratnasamy, B. Karp, S. Shenker, D. Estrin, R. Govindan, L. Yin, and F. Yu, "Data-centric storage in sensornets with GHT, a geographic hash table," *Proc. MONET*, vol. 8, no. 4, pp. 427–442, 2003.
- [3] B. Karp and H. T. Kung, "GPSR: Greedy perimeter stateless routing for wireless networks," presented at the ACM MOBICOM, Boston, MA, 2000.
- [4] J. Li, J. Jannotti, D. S. J. De Couto, D. R. Karger, and R. Morris, "A scalable location service for geographic ad hoc routing," in *Proc. ACM MOBICOM*, Boston, MA, Aug. 2000, pp. 120–130.
- [5] D. Niculescu and B. Nath, "Trajectory based forwarding and its applications," presented at the ACM MOBICOM, San Diego, CA, 2003.
- [6] J. Bicket, D. Aguayo, S. Biswas, and R. Morris, "Architecture and evaluation of an unplanned 802.11b mesh network," presented at the ACM MOBICOM, Cologne, Germany, 2005.
- [7] C. Perkins and P. Bhagwat, "Highly dynamic destination—Sequenced distance-vector routing (DSDV) for mobile computers," in *Proc. ACM SIGCOMM*, 1994, pp. 234–244.
- [8] S. Perkins and E. M. Royer, "Ad hoc on-demand distance vector routing," presented at the 2nd IEEE Workshop on Mobile Computing Systems and Applications, New Orleans, LA, Feb. 1999.
- [9] D. Johnson, D. Maltz, and J. Broch, C. E. Perkins, Ed., "DSR: the dynamic source routing protocol for multi-hop wireless ad hoc networks," in *Ad Hoc Networking*. Reading, MA: Addison-Wesley, 2001, ch. 5, pp. 139–172.
- [10] W. T. Tsai, C. V. Ramamoorthy, W. K. Tsai, and O. Nishiguchi, "An adaptive hierarchical routing protocol," *IEEE Trans. Comput.*, vol. 38, no. 8, pp. 1059–1075, Aug. 1989.
- [11] R. R. Choudhury and N. Vaidya, "Impact of directional antennas on ad hoc routing," presented at the 8th Int. Conf. Personal Wireless Communication (PWC), Venice, Italy, Sep. 2003.
- [12] R. Ramanathan, "On the performance of Ad Hoc networks using beam-forming antennas," presented at the ACM MobiHoc, Long Beach, CA, Oct. 2001.
- [13] S. Yi, Y. Pei, and S. Kalyanaraman, "On the capacity improvement of ad hoc wireless networks using directional antennas," in *Proc. ACM MobiHoc*, Annapolis, MD, Jun. 2003, pp. 108–116.
- [14] M. Yuksel, J. Akella, S. Kalyanaraman, and P. Dutta, "Free-space-optical mobile ad hoc networks: auto-configurable building blocks," *ACM/Springer Wireless Networks*, 2008, to be published.
- [15] D. Braginsky and D. Estrin, "Rumor routing algorithm for sensor networks," presented at the WSN Conf., Atlanta, GA, Oct. 2002.
- [16] T. He, C. Huang, B. M. Blum, J. A. Stankovic, and T. F. Abdelzaher, "Range-free localization schemes in large scale sensor networks," presented at the ACM MOBICOM, San Diego, CA, 2003.
- [17] D. Niculescu and B. Nath, "Ad hoc positioning system (APS) using AoA," presented at the IEEE INFOCOM, San Francisco, CA, 2003.
- [18] M. Gerla, X. Hong, and G. Pei, "Landmark routing for large ad hoc wireless networks," in *Proc. IEEE GLOBECOM*, Nov. 2000, pp. 1702–1706.
- [19] ns-2—The Network Simulator. [Online]. Available: <http://www.isi.edu/nsnam/ns>
- [20] MuniWireless. [Online]. Available: <http://www.muniwireless.com/>
- [21] D. S. J. De Couto, D. Aguayo, J. Bicket, and R. Morris, "A high-throughput path metric for multi-hop wireless routing," presented at the ACM MOBICOM, San Diego, CA, Sep. 2003.
- [22] S. M. Das, H. Pucha, and Y. C. Hu, "Performance comparison of scalable location services for geographic ad hoc routing," presented at the IEEE INFOCOM, Miami, FL, 2005.
- [23] T. Clausen and P. Jacquet, "OLSR," RFC 3626, Oct. 2003 [Online]. Available: <http://ietf.org/rfc/rfc3626.txt>
- [24] B. Chen and R. Morris, "L+: scalable landmark routing and address lookup for multi-hop wireless networks," MIT LCS, Cambridge, MA, Tech. Rep. 837, Mar. 2002.
- [25] M. Lim, J. Chesterfield, J. Crowcroft, and J. Chesterfield, "Landmark guided forwarding," in *Proc. 13th IEEE Int. Conf. Network Protocols (ICNP'05)*, 2005, pp. 169–178.
- [26] Z. Haas, J. Pearlman, and P. Samar, "The zone routing protocol (ZRP) for ad hoc networks," IETF Internet Draft, Jul. 2002.
- [27] M. Caesar, M. Castro, E. Nightingale, G. O'Shea, and A. Rowstron, "Virtual ring routing: Network routing inspired by DHTs," presented at the ACM SIGCOMM 2006, Pisa, Italy, Sep. 2006.
- [28] H. Pucha, S. M. Das, and Y. C. Hu, "Imposed route reuse in ad hoc network routing protocols using structured peer-to-peer overlay routing," *IEEE Trans. Parallel Distrib. Syst.*, vol. 17, no. 12, pp. 1452–1467, Dec. 2006.
- [29] A. Rao, S. Ratnasamy, C. Papadimitriou, S. Shenker, and I. Stoica, "Geographic routing without location information," presented at the ACM MOBICOM, San Diego, CA, 2003.
- [30] R. R. Choudhury and N. Vaidya, "Performance of ad hoc routing using directional antennas," *Ad Hoc Networks*, vol. 3, no. 2, pp. 157–173, Mar. 2005.
- [31] B. Leong, S. Mitra, and B. Liskov, "Path vector face routing: Geographic routing with local face information," *Proc. ICNP*, Nov. 2005, 12 pp.
- [32] S. Ratnasamy, B. Karp, L. Yin, F. Yu, D. Estrin, R. Govindan, and S. Shenker, "GHT: A geographic hash table for data-centric storage in sensornets," in *Proc. 1st ACM Int. Workshop on Wireless Sensor Networks and Applications (WSNA)*, Atlanta, GA, Sep. 2002, pp. 78–87.
- [33] R. R. Choudhury, X. Yang, R. Ramanathan, and N. H. Vaidya, "Using directional antennas for medium access control in ad hoc networks," in *Proc. ACM MobiCom*, Sep. 2002, pp. 59–70.
- [34] M. Sekido, M. Takata, M. Bandai, and T. Watanabe, "Directional NAV indicators and orthogonal routing for smart antenna based Ad Hoc networks," in *Proc. IEEE Int. Conf. Distributed Computing Systems Workshops*, Jun. 2005, pp. 871–877.



Bow-Nan Cheng (M'08) received the B.S. degree in electrical engineering from the University of Illinois at Urbana-Champaign, and the M.S. and Ph.D. degrees in computer systems engineering from Rensselaer Polytechnic Institute, Troy, NY, in 2005 and 2008, respectively.

He is a member of the Technical Staff at MIT Lincoln Laboratory. His research interests include routing using directional communications methods in hybrid free-space-optic (FSO) and RF disruption/delay tolerant wireless networks.

Dr. Cheng is a member of the ACM.



Murat Yuksel (M'02) received the B.S. degree in computer engineering from Ege University, Izmir, Turkey, and the M.S. and Ph.D. degrees in computer science from Rensselaer Polytechnic Institute, Troy, NY, in 1999 and 2002, respectively.

He is an Assistant Professor at the University of Nevada, Reno. His research is on various networking issues such as wireless routing, free-space-optical mobile ad hoc networks (FSO-MANET), network modeling and economics, protocol design, peer-to-peer, and performance analysis.

Dr. Yuksel is a member of the ACM and Sigma Xi.



Shivkumar Kalyanaraman (S'95–M'03–SM'07) received the B.Tech. degree in computer science from IIT Madras, India, and the M.S. and Ph.D. degrees from the Ohio State University, Columbus.

He is with IBM India Research Laboratory, Bangalore, India. He is a Professor (on leave) at the Department of Electrical, Computer and Systems Engineering at Rensselaer Polytechnic Institute, Troy, NY. His research interests include various traffic management topics and protocols for emerging tetherless networks.

He is a senior member of the ACM.